International Communications in Heat and Mass Transfer 164 (2025) 108819

Contents lists available at ScienceDirect

International Communications in Heat and Mass Transfer

journal homepage: www.elsevier.com/locate/ichmt

# Thermal performance and ageing effects to model the life cycle assessment of heat-protective thermal insulation materials in pipe systems

Ákos Lakatos [a,*], Attila Csík [b], Elena Lucchi [c], Angela Daniela La Rosa [d]

[a] University of Debrecen, Faculty of Engineering, Department of Building Services and Building Engineering, Ótemető Str 2-4, 4028 Debrecen, Hungary
[b] HUN-REN Institute for Nuclear Research, Bem tér 18/c, H-4026 Debrecen, Hungary
[c] Dipartimento di Ingegneria Civile e Architettura (DICAr), Università di Pavia, Via Ferrata 1, Pavia 27100, Italy
[d] Department of Manufacturing and Civil Engineering, Norwegian University of Science and Technology, Gjøvik 2815, Norway

ARTICLE INFO

*Keywords:*
Ceramic thermal insulations
Thermal conductivity
Heat treatment
LCA

ABSTRACT

Most power plants and district heating systems employ rock wool or ceramic fiberglass insulations to insulate their pipes. Over time, these materials lose some qualities. The present study tested two thermal insulation materials for applications in pipelines carrying hot steam in power plants or district heating (DH) systems: ceramic fiberglass (insulfrax) and flexible mineral wool. Thermal conductivity was measured at high temperatures (150 and 250 °C), simulating the effect of the passage of time. It was found that insulfrax had lower thermal conductivity in all cases 0.025–0.031 W/mK, compared to the mineral wool (0.038–0.422 W/mK). However, thermal conductivity of the mineral wool was continuously increasing (3 % and 9 %), and the thermal conductivity of the insulfrax jumped only after thermal annealing at 250 °C, but by about 24 %. Scanning electron microscopic imaging and differential scanning calorimetry experiments were used to reveal any possible changes in the structures of the materials after thermal annealing them at 150 and 250 °C for 1 day. The change in the specific heat was also calculated with differential scanning calorimetry, and crystallization processes were deduced. Finally, a comparative life cycle assessment was applied to select materials based on environmental performance, aligning with the Sustainable Development Goals requirements.

## 1. Introduction

The construction sector has recently garnered significant attention to their energy usage due to rising energy costs and consumptions [1]. In this context, reducing heat loss from pipe systems is essential for optimizing the energy performance and curbing carbon emissions of buildings [2–4]. Numerous studies highlight the potential of pipe systems to lower carbon footprints, particularly when coupled with advanced insulation materials and smart grid technologies. Pipelines play a critical role as conduits for thermal energy, facilitating the efficient and reliable transport of energy carriers, such as steam, hot water, or other heat-transferring media [3]. Heat pipes have high heat transfer capacities due to their high thermal conductivity (λ) and lack of mechanical structure [5]. Their insulation offers additional benefits related to condensation prevention, sound attenuation, safety enhancement, and fire resistance improvement [6]. Thus, optimizing thermal insulation is crucial for enhancing their overall performance and operation by minimizing heat loss and energy consumption and ensuring their structural integrity and thermal safety [7]. Also, it is crucial for maintaining a stable temperature of the fluid inside the pipes [8]. Pipe insulation is an important design consideration to ensure the energy efficiency of the building [9,10]. Summarizing, the thermal insulation of pipelines is crucial for several reasons:

- Reduction of heat loss: The pipeline system transports the high-temperature fluids through primary and secondary branches. Effective thermal insulation is critical to maximizing heat transfer efficiency. A higher λ of the pipe material leads to more significant heat loss, so an additional insulating layer is needed to minimize heat exchange between the fluid and the environment [7,11].
- Prevention of water condensation: Thermal insulation of the pipeline prevents condensation during temperature fluctuations, protecting the pipes from external corrosion [12].
- Protection against thermal burns: The insulation ensures that the outer surface of the pipe remains at a safe temperature, preventing accidental contact with hot pipelines [13,14].

* Corresponding author.
*E-mail address:* alakatos@eng.unideb.hu (Á. Lakatos).

https://doi.org/10.1016/j.icheatmasstransfer.2025.108819

Available online 7 March 2025

- Sound and noise attenuation: Insulated pipes mitigate noise from fluid flow and mechanical vibrations, contributing to a quieter operational environment [15].
- Fire protection: Insulation materials with fire-retardant properties help slow the spread of flames, improving the fire safety of the pipes [14].

Furthermore, the thermal efficiency of pipe systems can degrade over time due to physical deterioration, pipe corrosion, and mechanical damage to the thermal insulation material [15]. The insulation material can be artificially aged using heat treatments, ultraviolet (UV) or infrared (IR) radiation. These methods accelerate the kinetic processes and chemical and physical degradation, following an Arrhenius-type model that describes how temperature affects ageing processes:

$$t_a = \frac{ts}{2^{\left(\frac{Ta-Ts}{10}\right)}} \quad (1)$$

Wherein the ageing time ($t_a$) at a specific temperature ($T_a$) can be estimated based on the tested temperature ($T_s$) and the service time ($t_s$). Planning is heavily influenced by the λ factor's economic and operational endurance.

Material ageing causes gradual changes to its mechanical, thermal, and physical characteristics. Temperatures between the pipeline wall and the thermal insulation layer in nuclear power plants can reach 250 °C, altering the insulation's composition and λ. Prolonged exposure to high temperatures can induce physical changes in this material, such as shrinkage, embrittlement, or the formation of cracks. Also, high temperatures can weaken its mechanical properties, making it more susceptible to mechanical damage from vibrations, pressure changes, or other mechanical stresses. Mechanical damage and environmental exposure further compromise its effectiveness [16]. As pipes age, they lose insulating properties due to wear and environmental exposure, increasing heat loss [15]. Studies show that ageing insulation and physical deterioration can cause a reduction in thermal resistance (R), increasing the overall energy loss of the heating system [17] and energy demand [18]. Ageing infrastructure requires frequent maintenance and replacement, increasing operational costs and complicating energy management [9]. Pipe systems transport hot water through overground or underground pipes and often span large distances with large-diameter backbone lines and branches connecting various buildings. Many components of these systems (e.g., boilers, large fittings, and primary lines) are inadequately insulated despite operating at high temperatures [19]. The lack of proper insulation leads to significant issues: outdated primary transmission lines and incomplete thermal insulation result in substantial energy losses. Subject to environmental conditions, heat loss from exposed pipelines represents a considerable portion of industrial energy waste [20]. Insufficient thermal insulation incurs financial costs and exacerbates environmental impact through increased greenhouse gas emissions. In addition, poor insulation can cause condensation, corrosion, mold growth, and other pathogens, thereby increasing maintenance costs [21].

The selection of insulation materials is essential for preventing pipes' ageing. The criteria considered are low λ, high moisture resistance, reduced combustibility, high durability, cost-effectiveness, sustainability, and operating temperature range ($T_o$) around 250 °C [22; 23]. Common materials used in the past include: (i) mineral wool; (ii) Super Insulation Materials (SIMs); (iii) foam rubber wool; (iv) polyurethane foam (PUF). Flexible mineral wool has a λ of approximately 0.040 W/mK and a To from −180 °C to +700 °C. Thus, it is an excellent insulator for high-temperature applications. SIMs have λ of 0.015 W/mK and a $T_o$ = −60/+260 °C [21]. Particularly, inside theam insulfrax-type ceramic fibre are traditionally used for pipelines carrying hot steam. Foam rubber wool (λ ≅ 0.03 W/mK; $T_o$ = −200/+5 °C) and PUF (λ ≅ 0.02 W/mK; $T_o$ = −100/+150 °C) are no longer used due to their lower thermal resistance and limited high-temperature durability. Additionally, PUF is avoided because of the health risks associated with the toxicity of its components [20].

Otherwise, there is an increasing demand for materials with high resistance to fire [24–27], high temperatures [25], and thermal shocks [23,28], driven by the need for greater energy efficiency and reduced carbon emissions. Determining the optimal insulation thickness distribution systems requires the use of heat loss models to balance the reduction of environmental impacts [28], payback periods [29], and energy consumption [20]. Alternatively, insulation standards prescribe minimum thicknesses based on heat loss coefficients and pipe diameters to ensure compliance with thermal and energy efficiency regulations [20].

However, despite these advancements, there remain significant gaps in the literature regarding the optimal integration of insulation materials in varying environmental conditions and their long-term impacts on energy efficiency and sustainability:

- Long-term thermal performance studies assess how different insulation materials perform over extended periods in pipe systems. This includes evaluating λ stability, insulation effectiveness over time, and resistance to thermal degradation under varying environmental conditions (e.g., temperature fluctuations, humidity).
- Moisture resistance, absorption, retention, and its impact on thermal performance of insulation properties over time.
- Fire resistance and durability of insulation materials across the wide operational temperature range typically encountered in pipe systems considering material stability at both high and low temperatures and changes in insulation effectiveness under extreme conditions.
- Environmental impact and Life Cycle Assessment (LCA) to evaluate sustainability metrics and guide environmentally conscious material selection.

## 2. Aims

This multidisciplinary study aims to investigate the applicability and performance of two insulation materials (flexible mineral wool and insulfrax type ceramic fibre), as potential thermal insulators for pipelines carrying hot steam in power plants and pipe systems. These materials are considered suitable insulators for pipelines carrying hot steam for power plants or district heating systems [20]. As mentioned, these materials are specifically designed for excellent thermal resistance and minimal heat loss in high-temperature applications. Beyond thermal performance, other critical factors include moisture resistance, durability, and safety. Both materials are highly resistant to moisture absorption. This prevents degradation over time and extends the lifespan of insulated pipelines, even in environments with high air relative humidity or condensation. Their low combustibility is also essential for power plant settings where fire safety is a concern. Furthermore, their reduced combustibility makes them safer for industrial environments, where fire resistance is crucial. Thus, flexible mineral wool and insulfrax-type ceramic fibre were chosen because they offer the best combination of energy efficiency, durability, and fire resistance at high temperatures.

The study has the following objectives:

- Evaluate these materials' thermal stability and performance under high-temperature conditions, analyzing changes in λ and specific heat capacity after exposure to temperatures up to 250 °C.
- Examine how treatment affects the physical and structural integrity of the insulation materials through visual inspections, scanning electron microscopy (SEM), and differential scanning calorimetry (DSC) measurements.
- Explore the potential of these materials for use in high-temperature environments reaching up to 250 °C, evaluating their long-term viability, resistance to thermal ageing, chemical and physical degradation processes.

- Perform a comparative LCA to evaluate the environmental impact of the two suggested insulating systems.

The article's central questions are: (i) Does the material's appearance alter upon visual inspection due to heat treatment in an air environment? (ii) Does heat treatment affect the material's surface shape? (iii) Has the material's structure changed, and if so, how does this impact its thermal properties, such as its thermal conductivity? (iv) Can these materials be used in situations with higher temperatures? And finally, what system produces lower potential environmental impacts during the entire life cycle (including manufacturing, use and end-of-life).

## 3. Methodology

This study employs experimental techniques and analytical methods to evaluate the thermal and environmental performance and structural integrity of two fibrous insulation materials: flexible mineral wool and insulfrax ceramic fibre. The following steps outline the experimental procedures and data analyses conducted:

- Material selection and description (section 3.1).
- Sample preparation and thermal annealing (section 3.2).
- Analysis of the surface morphology (sections 3.3; 4.1), divided into:
  - o Visual inspection (sections 3.3.1; 4.1.1).
  - o Scanning Electron Microscopy (SEM) (sections 3.3.2; 4.1.2).
- Thermal performance measurements (sections 3.4; 4.2), divided into:
  - o Heat Flow Meter Measurements (HFM) (sections 3.4.1; 4.2.1).
  - o Differential scanning calorimetry (DSC) (sections 3.4.2; 4.2.2).
- LCA (section 5):
  - o Defining the functional unit suitable for the comparative analysis of the two materials.
  - o Evaluating the environmental impact from cradle to grave, including the life duration and the waste treatment for both systems.
  - o The experimental findings on thermal resistance and life duration for each material were used to calculate inventory data needed for the LCA analysis (such as the quantity of insulating material necessary for the application under study and the need for maintenance in the use phase).

### 3.1. Materials selection and description

As mentioned before, two fibrous insulation blankets were selected according to the suitability and applicability of proper pipe insulations:

- Flexible mineral wool (section 3.1.1).
- Insulfrax ceramic fibre blanket (section 3.1.2).

#### 3.1.1. Flexible mineral wool

Mineral wool, especially stone wool, is a commonly used thermal insulation material essential for preserving energy and containing fire development in structures thanks to its excellent temperature stability [22,30–35]. Furthermore, the air between the loosely connected mineral fibres gives such products outstanding heat and sound insulation. The most significant advantage of rockwool-based mineral wool insulation in Fig. 1a lies in its naturalness. Its base material is basalt stone, which remains durable even after processing. Rockwool-based mineral wool insulating elements do not shrink and retain their strength for decades because they hardly contain any organic substances but retain the favourable properties of basalt during production. First, the raw material, basalt, is ground to size and measured. It is then melted in a furnace at 1300–1400 °C, and fragile fibres with a 10–100 μm thickness are made from the liquid basalt using a centrifuge cylinder. The melt runs through a unique centrifuge cylinder line, where it draws fibres during cooling and enters the fibering chamber, where thermosetting synthetic resin is injected to bond the fibres mechanically, and impregnating oil is injected between the fibres to ensure water-repellent properties. The resulting fibres are then used to form a quilt, and the mineral wool is compacted using a particular technology. After that, the product is transferred to an oven, the thickness of which is fixed due to the baking. The finished quilt is then cut to size and packed. The oldest method of thermal insulation is to insulate the external pipes with ordinary or foil-wrapped mineral wool, and to tie the pipeline with a tape made of this material by fixing it with a binding wire. Mineral wool is produced in three types: (i) glass wool; (ii) stone wool; and (iii) slag. The first two types of materials fulfil most thermal insulation requirements: they have low λ, are inert to the insulated surface, possess sufficient flexibility, and demonstrate both chemical resistance and fireproof properties. Mineral wool can withstand temperatures up to 650 °C. Its advantages include excellent chemical resistance, non-toxic emissions ensuring safety for people, and low water absorption, which is crucial as moisture penetration can significantly reduce the effectiveness of any insulating material. Mineral wool materials can be vapour open and hydrophobic, they are usually covered with a hydrophobic agent. These properties make it suitable for a wide range of applications, with its high efficiency contributing to its widespread use. Due to these characteristics, it is used most to protect pipes from overheating. Additionally, the fibre-

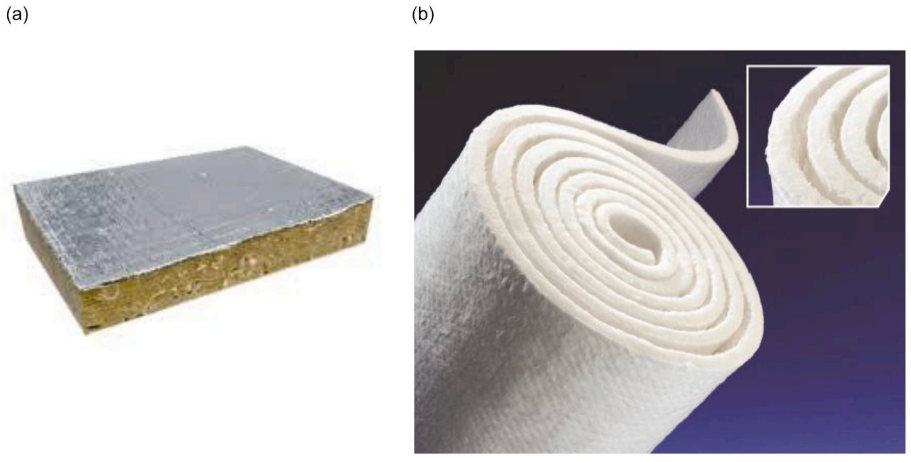


**Fig. 1.** a. Flexible mineral wool insulation.
b. Insulfrax ceramic fibre blanket insulation.

reinforced aluminium foil casing can safeguard the pipe shell from minor mechanical impacts and form a vapour barrier layer, preventing condensation or "sweating" on the outer surface of the pipe when insulating cold water pipes. It also meets fire protection class A1 standards.

#### 3.1.2. Insulfrax ceramic fibre blanket

Insulfrax blankets (Fig. 1b) are lightweight needle-felted blankets made from alkaline earth silicate (AES) wool. The material composition includes:(m%): $SiO_2$ 61,0–67,0; CaO 27,0–33,0; MgO 2,5–6,5; Al2O3 < 1,0; $Fe_2O_3$ < 0,6. These ceramic fibre blankets come in various roll widths, thicknesses, and densities, representing the next generation of low bio-persistent materials. Usually, they do not contain organic components that could contaminate high-temperature furnace atmospheres. Ceramic fibre blankets have the following characteristics: low λ, excellent resistance to thermal shock, and low heat storage capacity. These are important because the heat must be kept inside the transporting fluid in the pipe. Storing heat is not necessary for piping. Being entirely inorganic, they maintain strength, flexibility, and good thermal properties in various working environments without emitting smoke. Insulfrax S blankets are known for their exceptional handling, thermal shock resilience, high-temperature stability (up to 1200 °C), remarkable flexibility, and superb sound absorption. They are frequently employed as high-temperature insulation materials thanks to their superior thermal insulation capabilities and strong chemical stability. Typical applications include heat shields, mold covering insulation, pipe, sewer, and chimney insulation, passive fire protection, nuclear power plants, metallurgical industries, hypersonic vehicles, and channel linings for cogeneration and power plants. This is due to their unique structure, which gives them several benefits like high porosity, low density, large specific surface area, excellent thermal insulation performance, and thermodynamic stability performance [23,32–35]. They can reach a temperature range of up to 250 °C in these conditions.

### 3.2. Sample preparation and thermal annealing

The samples were prepared with the same base area 20 cm × 20 cm to have uniformity during the tests. The insulation λ value may alter due to the temperatures. These alterations could result from surface and structural material variations. Thermal annealing is crucial because it helps forecast the insulation's lifespan and application limit. It also acts as a thermal ageing process for the samples. Thus, to make the alterations visible, the samples were first heat annealed for one day at 150 °C and 250 °C separately in a Venticell 111 drying apparatus outside, for the heat treatments, new samples were used. This treatment accelerated ageing, allowing the observation of the effects of prolonged high-temperature exposure. We also kept the samples at 70 °C for a day after receiving them.

### 3.3. Analysis of the surface morphology

The heat annealing process can change the surface shape. The change may result from physical degradation, chemical reactions, or surface oxidation. The general surface morphology of fibre blankets can be considered a randomly distributed fibre network. The following experiments were conducted to verify the impact of the heat treatments on the samples' surface morphology: Visual inspection (section 3.3.1) and SEM (section 3.3.2).

#### 3.3.1. Visual inspection

Firstly, visual inspection through photo images was conducted to detect any apparent changes in the samples' physical appearance after

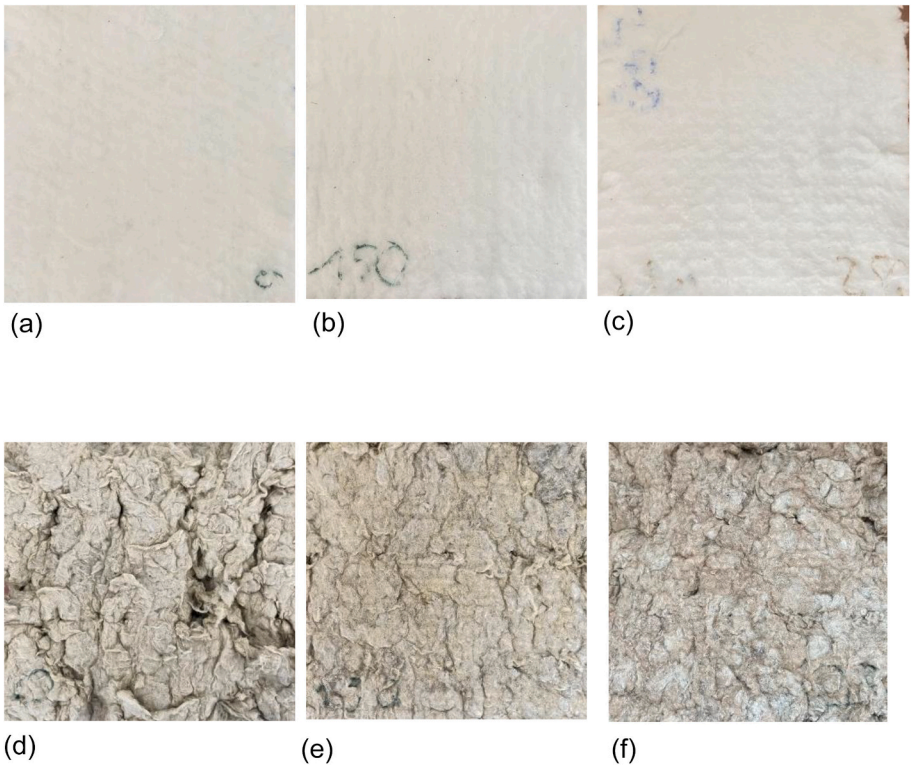


**Fig. 2.** a.Photo image of the un-annealed insulfrax sample.
b. Photo image of the annealed insulfrax sample for 1 day at 150 °C.
c. Photo image of the annealed insulfrax sample for 1 day at 250 °C.
d. Photo image of the un-annealed insulfrax sample.
e. Photo image of the annealed insulfrax sample for 1 day at 150 °C.
f. Photo image of the annealed insulfrax sample for 1 day at 250 °C

thermal annealing, these are presented in Fig. 2a to c.

#### 3.3.2. Scanning electron microscopy (SEM)

SEM was used to examine the surface morphology of the materials, identifying any microscopic alterations resulting from the heat treatments. A scanning electron microscope (LV-SEM, JEOL IT500HR) was used to gather surface morphological data from the samples that had been prepped and heated. The microscope ran at a 3 kV acceleration voltage to prevent charge accumulation. Utilizing such a modest acceleration voltage can primarily prevent the charging effect. Depending on the kind of material, the beam's penetration depth is generally between ten and hundreds of nm. This depth is usually in the range of 100 nm for SiO; the comparatively shallow penetration depth enabled the collection of more surface data. Secondary electron (SE) detection was used for topographic imaging of the materials with nanometer lateral resolution. A compositional analysis using a JEOL energy-dispersive X-ray (EDS) system with a 0.1 % detection threshold. The accelerating voltage was increased to 15 kV during the EDS measurement [36,37].

### 3.4. Thermal performance measurements

The heat annealing process can also change the thermal properties of the materials. The following measures were conducted: Heat Flow Meter Measurements (HFM) (section 3.4.1) and DSC (section 3.4.2).

#### 3.4.1. Heat flow meter measurements (HFM)

The HFM aimed to determine any changes in thermal conductivity due to heat treatment. The λ of the materials was measured using a Holometrix Lambda 2000 heat flow measuring device. This device provides accurate results with a relative error of about 5 % or less. The instrument operates according to ASTM C518 and ISO 8301 standards. Thus, as mentioned before (section 3.1) the materials were sized according to this dimension. To determine the λ coefficient of thermal insulation materials, the standard MSZ EN 12667:2001 was used as it applies to materials with medium and high λ resistance of at least $R = 0.5\ m^2K/W$. The calibration material used was a glass fibre standard tested by the US National Institute of Standards and Technology (NIST). Calibration ensures a measurement accuracy of 5 % or better. When there is a proper proportionality between the $U\Delta x/\Delta T$ and λ, the λ factor for an unknown specimen can be determined from the measured U and ΔT values, knowing the specimen's thickness.

Three pieces of 20 cm × 20 cm were prepared for the measurements from each thermal insulation material. A new untreated sample was used for each test. Initially, the λ of the wholly dried (70 °C for 1 day) sample was examined. Subsequently, the samples were heat treated at 150 °C and 250 °C for 1 day. Then, the λ of both heat-treated samples was measured. Five measurements were performed for each condition, and the average values of the results were calculated.

#### 3.4.2. Differential scanning calorimetry (DSC)

Most thermal insulation materials have an amorphous structure and contain a variety of oxides, including amorphous silica nanoparticles and silicon oxide. Due to the rise in temperature, the amorphous structure may reconfigure, crystallize, or recrystallize [38,39]. The crystallization process may compromise the materials' ability to act as thermal insulation, which can also cause an increase in heat conductivity. Thus, DSC measurements were conducted to analyze potential changes in the material's internal structure related to thermal transitions and stability under elevated temperatures. The technique assesses impurities and possible changes in the sample following heat supply.

After the powder in both samples was ground, their temperature sensitivity was measured using the Netzsch Sirius 3500 differential scanning calorimeter. A small amount (10 mg) from the samples was inspected. The measurement protocol involved heating the samples in a concave Al perforated lid from 30 to 300 °C at 10 °C per minute in an ambient and protective nitrogen environment, with a 40 and 60 ml/min flow rate, respectively. The DSC sign (in MW/mg) was recorded as a function of temperature to assess potential energy and structural alterations. Differential Scanning Calorimetry also calculated the change in the specific heat capacity.

The apparatus used for this measurement, a Netzsch DSC Sirius 3500 equipment, complies with DIN 51004, ISO 11357, ASTM E793, ASTM D3895, and ASTM D3418 standards.

## 4. Experimental results and discussion

The following test results are presented: 4.1) surface morphology analysis; 4.2) Thermal performance measurements.

### 4.1. Analysis of surface morphology

Changes in thermal properties and structural characteristics were correlated with the heat treatment temperatures to understand the degradation mechanisms according to Visual inspection and SEM techniques.

#### 4.1.1. Visual inspection

Visual inspection revealed that the colour of both Insulfrax (Figs. 2a to c) and mineral wool samples (Figs. 2d to f) darkened after thermal annealing, as shown in Figs. 2a to c. This colour change is likely due to the samples' surface oxidation. This discolouration can be explained by the fact that the heat treatment took place in atmospheric air. Fig. 2a (insulfrax) and 2d (mineral wool) belong to the un-annealed samples, while 2b (insulfrax) and 2e (mineral wool) and 2c (insulfrax) and 2f (mineral wool) show the annealed ones at 150 °C and 250 °C for 1 day, respectively. One can see from the rows that the darkest surface belongs to the samples annealed at 250 °C caused by the intensive surface oxidation (2c and 2f). The surface of the heat-treated samples after annealing them at 150 °C showed only a slight discolourization.

#### 4.1.2. Scanning electron microscope

SEM results are reported at three magnifications (150×, 450×, and 1400×). SEM photography effectively examines insulation sample surface morphology [33,40–43]. Pictures of the annealed and un-annealed insulfrax samples are shown in Figs. 3a–d. Fibrous insulation generally has the shape of small pipes covered with granules [44–47]. Here, the fibres reinforce the ceramic granules, which can be seen perfectly under high magnification at about 1400× in Fig. 3a. Based on the results of the scanning electron microscopic examination of the morphology of the insulating materials, it can be established that slight internal structural changes occur on the insulfrax sample. As the heat treatments progress, the fibres become smooth as the magnification increases. One can see from the images presenting 1400xX magnification that some grains disappear from the fibres.

Fig. 3d reflects the energy disperse element analysis, with the most contaminants of: Ca, C, O, Mg and Al, complete with silicon as a base material of the fibres.

It is visible in Fig. 3e by 1400× magnification that the mineral wool fibres are covered with the grains. The restructuration of the fibres is observed after thermal annealing. Fig. 3f and 3g present the SEM images of the mineral wool samples. It is also noticeable here that the granules and particles connected to the fibres fall.

Fig. 3h shows the contamination analysis, reached by energy dispersal element mapping. Mineral wool is based on silicon-oxide and is filled with C, Na, Mg, Ca, K, Al, Ti, and Fe. As a comparison of the SEM results of the two materials, one can state that the surface modification procedure due to the thermal annealing is the same for both materials. Thermal annealing makes the fibres' restructuration and the grains visible.

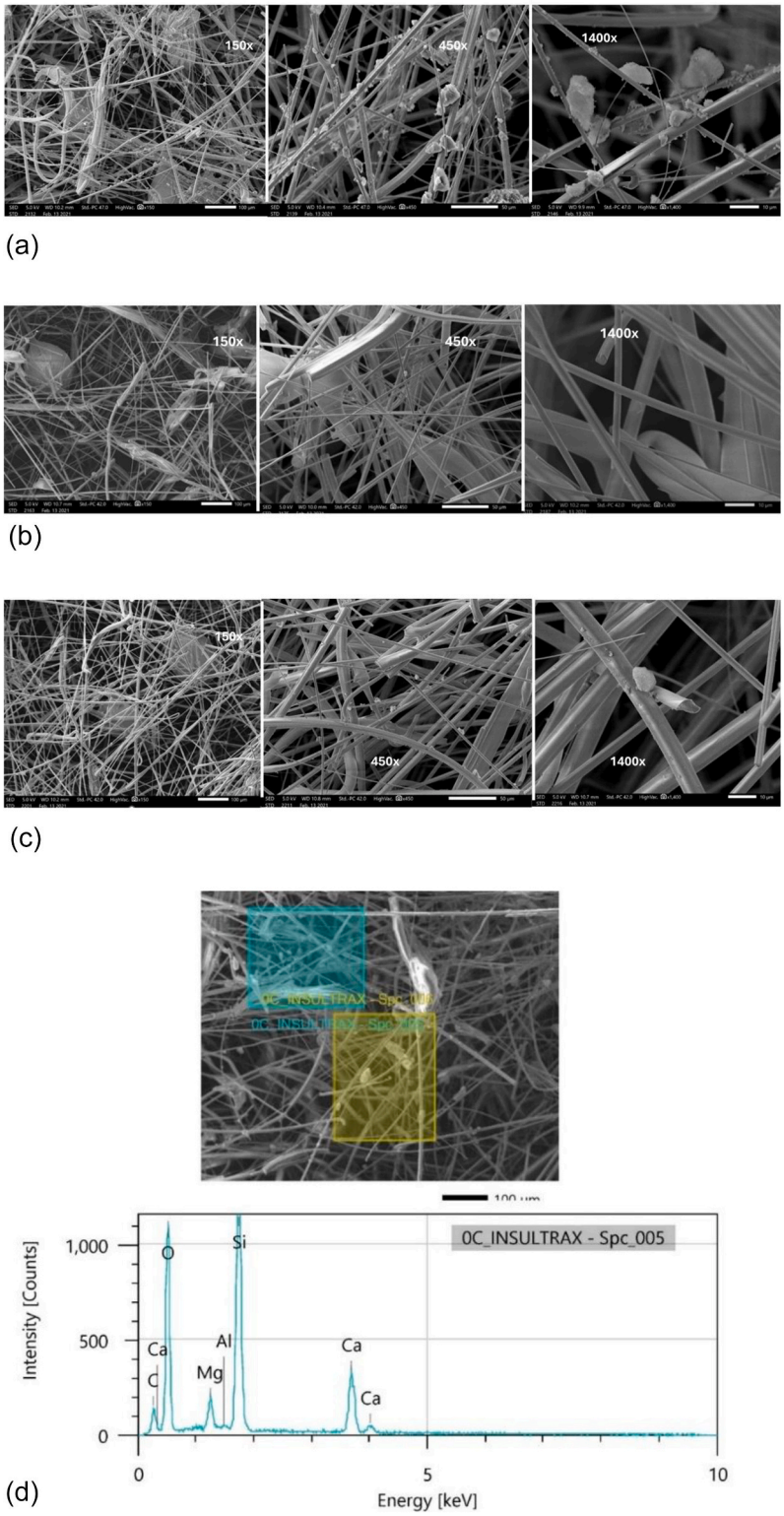


**Fig. 3.** a.The scanning electron microscope image of the un-annealed insulfrax sample with different magnifications (from left to right 150×, 450×, 1400×).
b. The scanning electron microscope image of the insulfrax sample annealed at 150 °C for 1 day with different magnifications (from left to right 150×, 450×, 1400×).
c. The scanning electron microscope image of the insulfrax sample annealed at 250 °C for 1 day with different magnifications (from left to right 150×, 450×, 1400×).
d. The EDS spectra and component intensity of insulfrax sample.
e. The scanning electron microscope image of the un-annealed mineral wool sample with different magnifications (from left to right 150×, 450×, 1400×).
f. The scanning electron microscope image of the mineral wool sample annealed at 150 °C for 1 day with different magnifications (from left to right 150×, 450×, 1400×).
g. The scanning electron microscope image of the mineral wool sample annealed at 250 °C for 1 day with different magnifications (from left to right 150×, 450×, 1400×).
h. The EDS spectra and component intensity of a mineral wool sample.

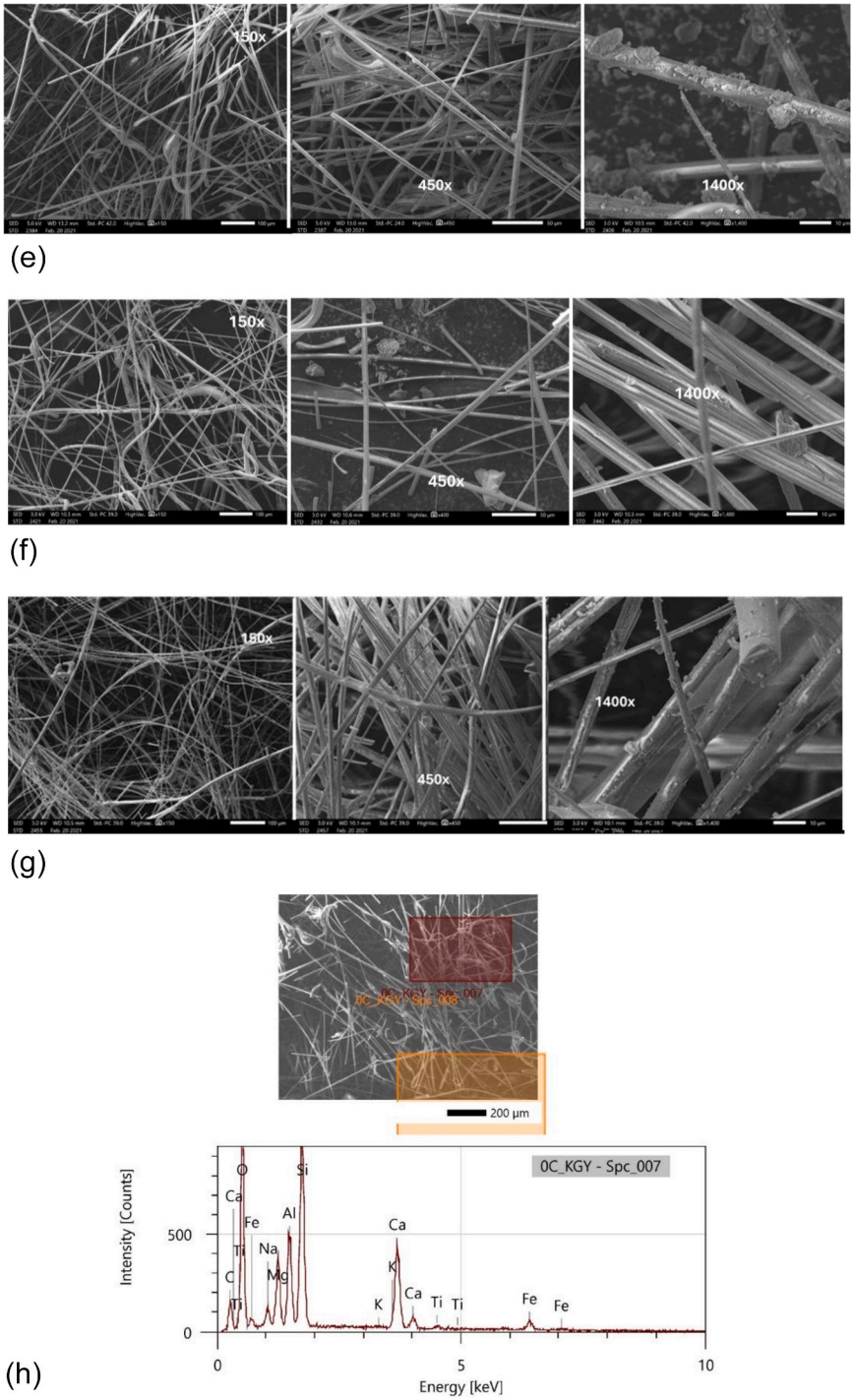


**Fig. 3.** (*continued*).

### 4.2. Thermal performance measurements

The materials' suitability for high-temperature applications was assessed based on their thermal performance and structural integrity post-annealing, according to the following tests: Heat Flow Meter Measurements (HFM) (section 4.2.1) and Differential scanning calorimetry (DSC) (section 4.2.2).

#### 4.2.1. Heat flow meter measurements (HFM)

The results of the λ measurements after the heat treatments performed on the samples were detailed. Fig. 4 presents the λ measurement results of the insulfrax and the mineral wool samples. It should be noted that the λ of the mineral wool was measured without the alumina cashiering.

The graphical representation of insulfrax in Fig. 4 (indicated by white squares) demonstrates that the measured λ is stable, maintaining an almost constant value until the heat treatment at 150 °C. Following heat treatment at 250 °C, the λ increases by approximately 24 %. Furthermore, the measured λ of the untreated sample aligns with the value provided by the manufacturer. SiO2 particles were identified on some of the glass fibres for non-heat-treated samples. Like aerogel-containing insulators, these particles flaked off due to heat treatment. However, the quantity of these particles is minimal, and their impact on the heat conduction properties is negligible.

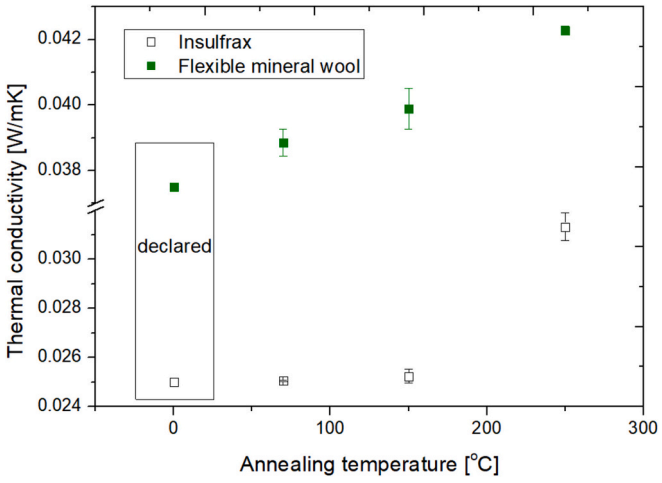


**Fig. 4.** Thermal conductivity measurement result.

Moreover, for the mineral wool, it is also evident from the graphic representation that the measured thermal conductivity of the materials increases, but the thermal conductivity of the untreated sample shows a value close to the manufacturer's value. As we measured, the thermal conductivity of the samples heat-treated at 250 °C shows a change of about 10 % compared to the thermal conductivity of the untreated sample. The images taken of the samples show that the external surface of the samples changes due to heat treatment.

To put it all in a frame, we can mention that insulfrax had lower thermal conductivity in all cases 0.025–0.031 W/mK, compared to the mineral wool (0.038–0.422 W/mK). However, the thermal conductivity of the mineral wool was continuously increasing (3 % and 9 %), and the thermal conductivity of the insulfrax jumped only after thermal annealing at 250 °C, but by about 24 %. For the tests with insulfrax, a thickness of 2.6 cm was used, while the mineral wool samples with 4.4 cm in thickness were used. The reason for this was the availability of the samples on the market. These two thicknesses are typical. Here, it has to be mentioned that based on the EDS analysis of the samples (Fig. 3 d and h) mineral wool contains more metallic components such as Fe and Ti, which can result in a higher thermal conductivity. Moreover, it can also result in higher thermal stability and less change (9 %) in the thermal conductivity after thermal annealing.

Here, it has to be mentioned that the material with lower thermal conductivity can fulfil the requirements (if there are) in smaller thicknesses.

#### 4.2.2. *Differential scanning calorimetry (DSC)*

For the insulfrax, we found that the profile has a half-gaussian shape until a peak at 300 °C, which can be seen in Fig. 5a. Here, a possible slight crystallization with dehumidification can be expected. Generally, the crystallization process increases the thermal conductivity of the materials because both the crystalline phase and parallel free electrons enhance heat conduction. One can deduce here a change in the specific heat capacity with about 1440 J/kgK value.

Similar results can be found presented in Fig. 5b for mineral wool. Starting from room temperature, a similar half-gaussian shape is observable, but the peak is at 250 °C. The change in the specific heat capacity is about 1250 J/kgK. The monotonic increase in the DSC sign can similarly lead to the rise in thermal conductivity presented earlier. Increasing $C_p$ value might belong to crystallization.

#### 4.2.3. *Shrinkage and compressibility tests*

Another essential requirement of the materials used for pipes is their flexibility, as well as their shrinkage. Shrinkage can predict durability. Due to the structural changes, if the material shrinks quickly, its lifetime

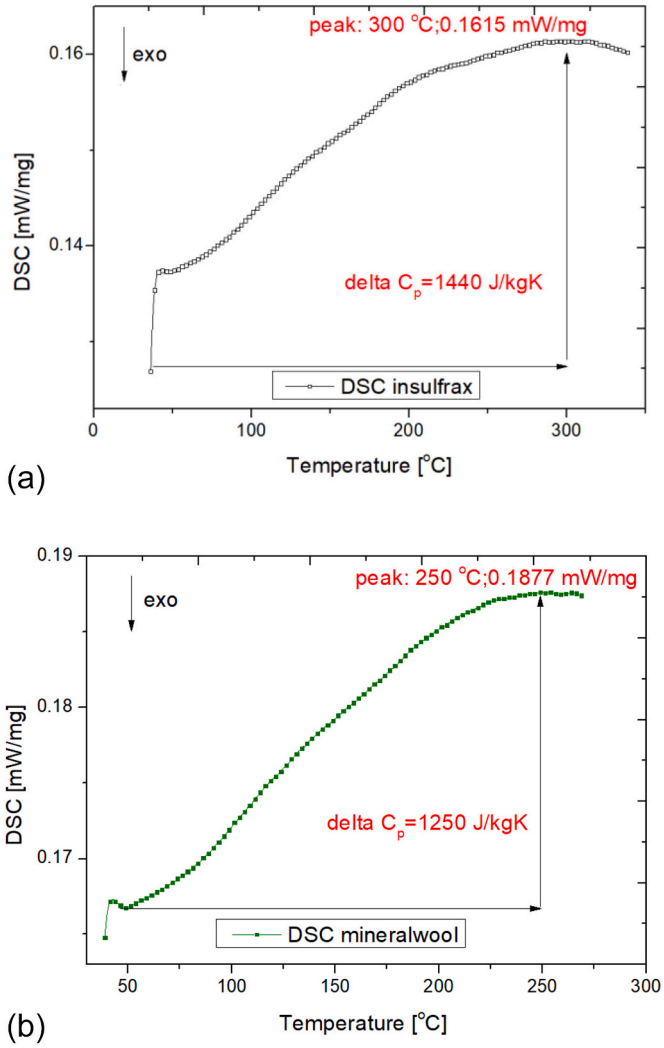


**Fig. 5.** a.The DSC curve of the insulfrax sample.
b. The DSC curve of the mineral wool sample.

can be shorter. Moreover, suppose the thickness becomes lower due to ageing over time. In that case, the thermal resistance decreases, so the material can lose the initial thermal resistance and will no longer meet the design value. We applied a compressibility test on the material as follows to check this. From the tested samples, we also prepared ones with 20 cm × 20 cm geometries, which were subjected to different loads between 0 and 15 kPa with Netzsch equipment. As a result, we investigated the changes in the thickness and density of the materials. Conducting this experiment is justified because the insulation cannot be attached to pipelines transporting hot media by glueing but only by mechanical fastening with caulking (secondary branch) or by fastening with other fiberglass material (primary branch). This may mean deformation in the material, resulting in a deviation from the design values. The figures below show the effect of different loads on the materials. From the statistics above, it can be concluded that the thickness of rockwool insulation decreases by at least 50 % even at the lowest load and by almost 80 % at the highest load, which can cause a significant difference between design and construction. The exact change for Insulfrax thermal insulation means 35 % and 55 % presented in Figs. 6 a and b.

#### 4.2.4. *Thermal resistance and heat loss calculations*

Thermal conductance and thermal resistance are essential concepts in thermodynamics, thermal engineering, and heat transfer that char-

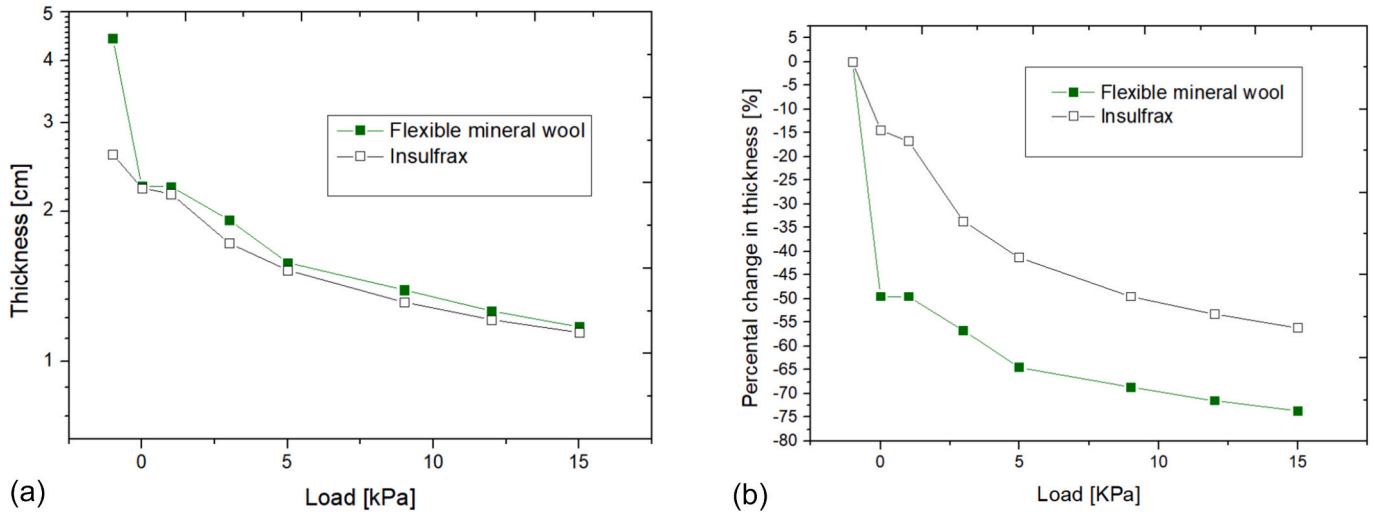


**Fig. 6.** a. Load vs Thickness.
b. Load vs. percental change in the thickness.

acterize a material's or system's capacity to carry heat and the resistance it provides to the heat current. By adjusting these characteristics, engineers can regulate temperature gradient, avoid thermal shock, and increase thermal system efficiency. Thermal resistance allows two to compare the thermal insulation capability of different materials. It depends on the specimen's thermal conductivity and thickness/diameter. The thermal resistance equals the heat loss ratio and the temperature difference. If we suppose a cylindrical shape (heat transfer through a multilayered pipe) with external and internal fluid flow, the thermal resistances can be calculated by using Eq.2, 3, 4 and 5, where $R_i$ and $R_e$ are the surface heat transfer resistances between the solid body and the flowing fluid, moreover, $\alpha_i$ and $\alpha_e$ are the internal (index:i) and external (index:e) surface heat transfer coefficients (12 and 5800 W/m$^2$K), moreover d in cm is the diamater.

$$R_i = \frac{1}{d_i \bullet \pi \bullet \alpha_i} \tag{2}$$

$$R_e = \frac{1}{d_e \bullet \pi \bullet \alpha_e} \tag{3}$$

$R_1$ gives the thermal resistance of the pipe, while $R_2$ represents the thermal resistance of the insulations.

$$R_1 = \frac{1}{2 \bullet \pi \bullet \lambda_1} ln\frac{d_e}{d_i} \tag{4}$$

$$R_2 = \frac{1}{2 \bullet \pi \bullet \lambda_{insulation}} ln\frac{D_{insulation}}{d_e} \tag{5}$$

To compare the thermal insulation capability of the tested materials, we calculated a possible heat transfer rate (q in W/m) value through a steel pipe with $d_e = 25$ mm and $d_i = 20$ mm diameters, hypothetically. We calculated the heat transfer rate without insulation using Eq.6 and in insulated cases by using the lambda values of the insulfrax and mineral wool measured after thermal treatment by using Eq.7. We suppose that the pipe transports hot water/steam fluid with different temperatures ($T_i = 70$, 150 and 250 °C). We also calculated a design state using the thermal conductivities of insulfrax and mineral wool given by the manufacturers at $T_i = 10$ oC. $\lambda_1 = 50$ W/mK was the thermal conductivity of a steel pipe.

where $D_{insulation} = 2 \times 2.6$ cm for the insulfrax and $2 \times 4.4$ cm for the mineral wool; $T_i$ is the external temperature fixed to 0 °C.

$$q_{no\ insulation} = \frac{T_i - T_e}{\frac{1}{d_i \bullet \pi \bullet \alpha_i} + \frac{1}{2 \bullet \pi \bullet \lambda_1} \bullet ln\frac{d_e}{d_i} + \frac{1}{d_e \bullet \pi \bullet \alpha_e}} \tag{6}$$

$$q_{ins} = \frac{T_i - T_e}{\frac{1}{d_i \bullet \pi \bullet \alpha_i} + \frac{1}{2 \bullet \pi \bullet \lambda_1} \bullet ln\frac{d_e}{d_i} + \frac{1}{2 \bullet \pi \bullet \lambda_{insulation}} \bullet ln\frac{D_{insulation}}{d_e} + \frac{1}{D_{insulation} \bullet \pi \bullet \alpha_e}} \tag{7}$$

The results of the above calculations are collected in Table 1 where the benefit of insulfrax insulation is highlighted by the more significant heat reduction compared to mineral wool. The heat reduction for insulfrax is between 705 and 569 %, while using the mineral wool, the heat ranges between 615 and 555 %.

### 4.2.5. *Lifetime calculation*

Using Eq. 1, one can estimate the lifetime of the samples after annealing them. With this equation, one can calculate the ageing of the samples. It must be mentioned that it can be used cautiously, where one will not get long service times. If one considers the service temperature to 10 °C, common in building energetics, one can find the 1 day thermal annealing at 70 °C to be 64 days, while the thermal treatment at 150 °C gives a service time at 10 °C to 45 years. It has to be mentioned that this equation provides unuseful results over 150 °C. Moreover, we can

**Table 1**
The results of the heat transfer calculations.

| | | $T_e = 0$ °C | $T_i$ design | $T_{i1}$ | $T_{i2}$ | $T_{i3}$ |
|---|---|---|---|---|---|---|
| | | | 10 °C | 70 °C | 150 °C | 250 °C |
| | $R_i$ [mK/W] | | 0.0027 | | | |
| | $R_1$ [mK/W] | | 0.0007 | | | |
| Resistance without insulation | $R_e$ [mK/W] | | 1.0616 | | | |
| Heat flow without insulation | q [W/m] | | 9.39 | 65.73 | 140.84 | 234.74 |
| Mineral wool resistance | $R_2$ [mK/W] | | 6.3213 | 6.1830 | 6.0218 | 5.6821 |
| Mineral wool resistance | $R_e$ [mK/W] | | 0.2349 | | | |
| Mineral wool heat flow | q [W/m] | | 1.52 | 10.90 | 23.96 | 42.23 |
| Percental reduce [%] | | | 615.91 | 602.92 | 587.79 | 555.89 |
| Insulfrax resistance | $R_2$ [mK/W] | | 7.1652 | 7.1652 | 7.0998 | 5.7193 |
| Insulfrax resistance external surface | $R_e$ [mK/W] | | 0.3447 | | | |
| Insulfrax heat loss | q [W/m] | | 1.33 | 9.32 | ***20.14*** | 41.20 |
| Percental reduce [%] | | | 705.45 | 705.45 | 699.32 | 569.70 |

emphasize from the DSC curves that both materials suffer structural change over 200 °C. For this, we can conclude that the insulfrax is stable (with constant thermal conductivity) till 150 °C, for about 45 years at a service temperature of 10 °C. Over this, its thermal conductivity changes by about 24 %. Regarding mineral wool, we can state that the thermal conductivity slightly increased, with about 3 % and 9 %.

## 5. Life cycle assessment (LCA)

### 5.1. LCA methodology

The comparative LCA analysis used the amount of insulating material needed to reach a specific insulating performance required for the application in the heat district pipe system. Following the standardized methodology (ISO 14040-44), there are four phases: 1.Goal & Scope; 2. Life Cycle Inventory (LCI); 3. Life Cycle Impact Assessment (LCIA) and 4. Interpretations were included in the analysis [48,49]. The four phases are illustrated in Fig. 7.

#### 5.1.1. Goal and scope definition

The goal and scope phase defines the study and describes the why and how for the analysis to ensure consistency in the LCA. As LCA gives a model of a complex reality, simplifying is necessary. A carefully defined goal and scope minimizes the influence and distortion of the results. Additionally, the most important choices made in the LCA are described here. The intended application of the product, process or service should be described in the goal, along with the reasons for the study, the intended audience and to whom the analysis will be disclosed. The product system studied the system's function or systems, should be described in the scope. The functional unit, which describes the system's function, is described in this section. All inputs and outputs are considered concerning this functional unit and are normalized to this. The system boundaries define what should be included and left out of the study and are also part of the scope. The allocation procedure is described, to explain how the impacts are allocated based on choices made. Methodology and impact categories are also described in the scope, along with data requirements, assumptions, and limitations [51].

#### 5.1.2. Inventory analysis (LCI)

The second phase of LCA is the inventory analysis. Data collection of all environmental inputs and outputs are listed in an inventory. Environmental inputs refer to anything taken from the environment and added to the life cycle. In contrast, environmental outputs are taken from the product's life cycle and added to the environment [51]. The inventory analysis can be considered in four steps: preparing for data collection, data collection, calculation, and allocation. The source's reliability must be documented, as this gives the reliability of the data collected.

#### 5.1.3. Life cycle impact assessment (LCIA)

Impact assessment is the third phase of LCA. The impact potentials are found in the inventory. These are divided into different categories using impact assessment methods. There are two overall categories: midpoint and endpoint. Midpoint categories focus on single environmental problems, while endpoints focus on three protection areas. These areas are human health, ecosystem, and resources. The effects of midpoint categories are collected and categorized into the endpoint categories.

#### 5.1.4. Interpretation

Interpretation is the fourth and final phase of the LCA. The results are interpreted concerning the goal and scope to ensure consistency, and conclusions are made and checked to be well substantiated. The completeness, sensitivity, and accuracy of the data. If the data is incomplete, justifications and explanations should also be made in this phase.

### 5.2. Comparative LCA of the selected materials

A comparative LCA was conducted among the two materials under study: mineral wool and insulfrax, with dimensions of the panels 20 cm x20cm.

The Ecoinvent database and the Simapro software were adopted for the assessment. For the mineral wool inventory, the data available for stone wool were taken directly from the Ecoinvent database. For the Insulfrax insulating material, according to the product information sheet [52] it is made of "man-made"2 vitreous (silicate) fibre with random orientation with alkaline oxide and alkaline earth oxide content greater than 18 % by weight. The Ecoinvent database does not provide this data, so the proxy data "glass fibre" was taken.

#### 5.2.1. Functional unit definition and inventory data modelling

The functional unit (FU) was an insulating panel with a specific thermal resistance (20,14 W/m) for district heating pipe applications.

Thermal conductivity was used as a critical parameter to calculate the optimized amount of each material needed to fulfil the thermal resistance defined in the FU.

According to the experimental results reported in the paragraph, Insulfrax had lower thermal conductivity λ (that means higher thermal resistance) in all temperature profiles (0.025–0.031 W/mK) compared

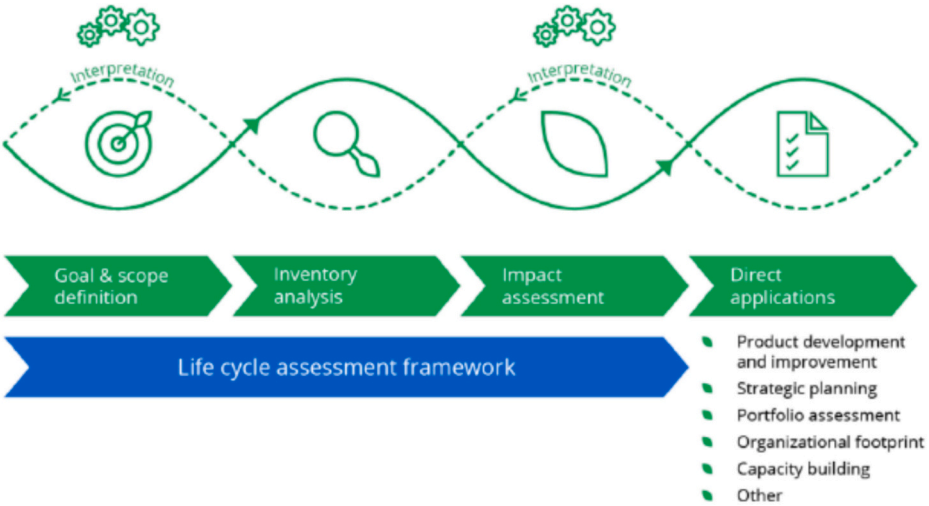


**Fig. 7.** The stages of a life cycle assessment are based on ISO14040 and 14,044 [50].

to the mineral wool (0.038–0.422 W/mK).

With Eq. 8, we calculated the required insulation thickness for the mineral wool to reach this thermal resistance of 20.14 W/m.

$$\frac{1}{2 \bullet \pi \bullet \lambda_{insulation}} \bullet ln\frac{D_{insulation}}{d_e} + \frac{1}{D_{insulation} \bullet \pi \bullet \alpha_e} = \frac{T_i - T_e}{q_{ins}} - (R_i + R_1) \quad (8)$$

It was calculated that the optimized mineral wool panel thickness should be $D_{insulation} = 6$ cm (from Eq.8) while the Insulfrax panel's thickness is 2.6 cm.

Inventory data used for the impact assessment are reported in Table 2.

To assess the inventory data for the use phase, shrinkage and compressibility tests were conducted as they can predict the durability. Due to the structural changes, if the material shrinks easily, its lifetime can be shorter. Moreover, suppose the thickness becomes lower due to ageing by time. In that case, the thermal resistance decreases, so the material can lose the initial thermal resistance and will no longer meet the design value. Further analysis will be dedicated to predicting the insulating materials' durability at high temperatures as more experimental tests are required to reach this goal. Therefore, the use phase was not included in the current LCA system boundary.

### 5.2.2. Impact assessment

The impact assessment was conducted using the CML-IA method, developed by the Center of Environmental Science (CML) of Leiden University in The Netherlands [53]. Results reported in Fig. 8a concern the production of 1 kg of each material (Insulfrax and mineral wool).

It is evident from Fig. 8a that the production of Insulfrax generates higher impacts for all the impact categories assessed by the CML method. However, when thermal conductivity is used to optimize the weight of material needed to reach the requested thermal resistance, the weight of Insulfrax is lower than that of mineral wool. Consequently, the environmental impact assessed in the manufacturing phase is lower for Insulfrax (Fig. 8b).

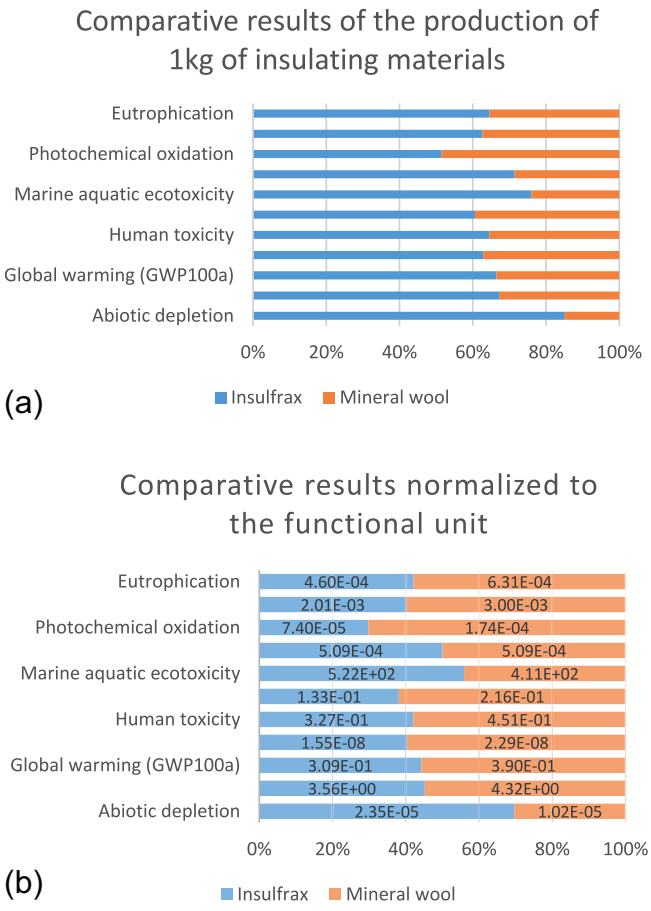


**Fig. 8.** a.Comparative impact results of the production of 1 kg of insulating materials.
b. Comparative impact results normalized to the functional unit.

## 6. Conclusions

This article analyses two fibrous thermal insulation materials (insulfrax and mineral wool). The change in their thermal and structural parameters was tested during the research. The thermal conductivities of the as-received (un-annealed) samples were measured using a heat flow meter. Moreover, this material constant was also tested after thermal annealing at 150 °C and 250 °C for 1 day, representing the resistance of the materials due to time. A further reason of thermal annealing is to discover the applicability limit of these materials because they are used for insulating pipes transporting hot water.

We deduced that the insulfrax kept its thermal conductivity at 0.025 W/mK till 150 °C and over it changed. In contrast, the thermal conductivity of the mineral wool was slightly changed, but it continuously changed from 0.038 W/mK, with an overall change of only 3 %.

After these, the samples' surfaces were also tested with a scanning electron microscope, and we stated that the surface modification procedure due to the thermal annealing was the same for both materials. Thermal annealing makes the fibres' restructuration and the grains visible. Pure powdered samples were also tested with a differential scanning calorimeter to see the continuous effect of heat treatment between 30 °C and 300 °C. It showed a linear increase in the specific heat capacity of both materials, predicting crystallization processes, which can increase thermal conductivity.

Moreover, experimental results were used to model the inventory data needed for the LCA. The weight of 312 g for mineral wool and 124.8 g of insulfrax was calculated to guarantee the same thermal resistance. In the manufacturing phase, these results led to a lower environmental impact associated with Insulfrax. Further analysis will be dedicated to predicting the insulating materials' durability at high temperatures as more experimental tests are required to reach this goal.

**Table 2**
Data used for the calculation of the optimized weight of insulating material.

| Selected materials | Mineral wool | Insulfrax |
|---|---|---|
| Thermal conductivity (W/mK) (laboratory value measured near room temperature) | 0.038 | 0.025 |
| Insulating panel dimensions (cm) | 20 × 20 | 20 × 20 |
| Optimized thickness (cm) | 6 | 2.6 |
| Density (kg/m$^3$) | 130 | 120 |
| Weight of insulating material needed to fulfil the FU thermal resistance requirements (gr) | 312 | 124.8 |

## CRediT authorship contribution statement

**Ákos Lakatos:** Writing – review & editing, Writing – original draft, Supervision, Project administration, Methodology, Investigation, Funding acquisition, Formal analysis, Data curation, Conceptualization. **Attila Csík:** Writing – review & editing, Methodology, Investigation, Data curation. **Elena Lucchi:** Writing – review & editing, Writing – original draft, Methodology, Investigation, Data curation, Conceptualization. **Angela Daniela La Rosa:** Writing – review & editing, Writing – original draft, Validation, Methodology, Investigation, Formal analysis, Data curation, Conceptualization.

## Declaration of competing interest

The authors declare that they have no known competing financial interests/personal relationships that could have appeared to influence

the work reported in this paper.

## Data availability

Data will be made available on request.

## Acknowledgements

Project no. TKP2021-NKTA-34 has been implemented with the support provided by the Ministry of Innovation and Technology of Hungary from the National Research, Development and Innovation Fund, financed under the TKP2021-NKTA funding scheme.

## References

[1] O. Kaynakli, A study on residential heating energy requirement and optimum insulation thickness, Renew. Energy 33 (2008) 1164e1172.
[2] A. Volkova, E. Latosov, K. Lepiksaar, A. Siirde, Planning of district heating regions in Estonia, Int. J. Sustain. Energy Plann. Manag. 27 (2020) 5–15.
[3] Mengke Jing, Shujie Zhang, Fu Lisong, Guoquan Cao, Rui Wang, Reducing heat losses from aging district heating pipes by using, cured-in-place pipe liners, Energy 273 (2023) 127260.
[4] H. Lund, B. Moeller, B.V. Mathiesen, A.J.E. Dyrelund, The role of district heating in future renewable energy systems, Energy 35 (3) (2010) 1381–1390.
[5] H. Jouhara, et al., Investigation on a full-scale heat pipe heat exchanger in the ceramics industry for waste heat recovery, Energy 223 (2021) 120037.
[6] F. Domhagen, B. Adl-Zarrabi, Influence of oxidation on radiative heat transfer in polyurethane insulation used for district heating pipes, Energy Procedia 132 (2017) 309–314.
[7] L. Zhang, et al., Design and optimization of thermal insulation structure for high-temperature pipeline inside the lower tank wall, Ann. Nucl. Energy 192 (2023) 109988.
[8] A. Keçebas, M.A. Alkan, M. Bayhan, Thermo-economic analysis of pipe insulation for district heating piping systems, Appl. Therm. Eng. 31 (2011) 3929e3937.
[9] H. Lund, et al., The role of district heating in future renewable energy systems, Energy 35 (3) (2010) 1381–1390.
[10] F. Lu, M. Kaviany, J. Williams, Thomas Addison-Smith, Heat, mass and momentum transport in wet mineral-wool insulation: experiment and simulation, Int. J. Heat Mass Transf. 228 (2024) 125644.
[11] Song He, Wu Xiya, Xiaoqian Zhang, Junwei Sun, Fuliang Tian, Saiping Guo, Du Haipeng, Ping Li, Yajun Huang, Preparation and properties of thermal insulation coating based on silica aerogel, Energ. Build. 298 (2023) 113556.
[12] A.K.I.N. Süleyman Kamil, Mustafa Alptekin, Examining the performance of thermal insulation materials used in buildings for noise insulation, Case Stud. Therm. Eng. 51 (2023) 103556.
[13] M. Nowak-Ocło'n, P. Ocło'n, Thermal and economic analysis of preinsulated and twin-pipe heat network operation, Energy 193 (2020) 116619.
[14] I.A. Zakirova, N.D. Chichirova, An investigation of thermal processes in insulation with a thin-film coating on heating network piping, Therm. Eng. 66 (10) (2019) 737–743.
[15] M. Perpar, Z. Rek, The ability of a soil temperature gradient-based methodology to detect leaks from pipelines in buried district heating channels, Energies 14 (18) (2021) 5712.
[16] Á. Lakatos, F. Kalmár, I. Csáky, Material selection in order to minimize the heat loss of piping based on measurements and calculations, AIP Conf. Proc. 2186 (2019) 070011.
[17] Lid'en P, Adl-Zarrabi B, Hagentoft C-E., Diagnostic protocol for thermal performance of district heating pipes in operation. Part 2: estimation of present thermal conductivity in aged pipe insulation, Energies 14(17):5302 (2021).
[18] S. Hámori, F. Kalmár, Hydraulic balancing analysis of a central heating system with constant supply temperature, Environ. Eng. Manag. J. 13 (11) (2014) 2789–2795.
[19] G. Eleftheriadis, M.M. Hamdy, The impact of insulation and HVAC degradation on overall building energy performance: a case study, Buildings 8 (2) (2018) 1–11.
[20] S. El Mrabet, et al., A brief overview of district heating pipe network progress, Energy Convers. Manag. 23 (2024) 100641.
[21] A. Lakatos, E. Lucchi, Thermal performances of super insulation materials (SIMs): a comprehensive analysis of characteristics, heat transfer mechanisms, laboratory tests, and experimental comparisons, Int. Commun. Heat Mass Transf. 152 (2024) 107293.
[22] P.G. Jensen, L. Belmonte, M. Solvang, Y. Yue, Quantification of high temperature stability of mineral wool for fire-safe insulation, J. Non-Cryst. Solids 622 (2023) 122680.
[23] K. Daryabeigi, Analysis and testing of high temperature fibrous insulation for reusable launch vehicles, J. Aiaa J. 1 (1999) 179–184.
[24] S. Li, X. Zhang, X. Cheng, G. Han, Y. Si, Y.-T. Liu, J. Yu, B. Ding, Flexible and compressive Al2O3/ZrO2/Y2O3 nanofibrous membranes for thermal insulation at 1400 °C, Compos. Commun. 35 (2022) 101290.
[25] A. Lu, J.N. Armstrong, H. Yong, H. Yulong, L. Zheng, Z. Donghui, S. Jesse, G. Zipeng, Z. Chi, R. Shenqiang, High temperature ceramic thermal insulation material, Nano Res. 15 (2022) 6662–6669.
[26] X. Zhang, Q. Tian, B. Wang, N. Wu, C. Han, X. Long, Y. Wang, Flexible porous SiZrOC ultrafine fibers for high-temperature thermal insulation, Mater. Lett. 299 (2021) 130131.
[27] X. Mao, L. Zhao, K. Zhang, Y.Y. Wang, B. Ding, Highly flexible ceramic nanofibrous membranes for superior thermal insulation and fire retardancy, Nano Res. 15 (2022) 7.
[28] Y. Başoğul, C. Demircan, A. Keçebaş, Determination of optimum insulation thickness for environmental impact reduction of pipe insulation, Appl. Therm. Eng. 101 (2016) 121–130.
[29] F. Li, P. Jie, Z. Fang, Z. Wen, Determining the optimum economic insulation thickness of double pipes buried in the soil for district heating systems, Front. Energy 15 (2021) 170–185.
[30] A. Lakatos, Thermal insulation capability of nanostructured insulations and their combination as hybrid insulation systems, Case Stud. Therm. Eng. 41 (2023) 102630.
[31] Kestutis Miskinisa, Vidmantas Dikaviciusa, Andrius Buskab, Karolis Banionisa, Influence of EPS, mineral wool and plaster layers on sound and thermal insulation of a wall: a case study, Appl. Acoust. 137 (2018) 62–68.
[32] Zhicheng Zhou, Qu Jian, Tao Zhang, Qin Sun, Effect of heat leakage on the operational characteristics of two-phase loop thermosyphon with a thermal insulation pipe, Int. J. Heat Mass Transf. 196 (2022) 123224.
[33] Yueqi Shao, Xu Jie, Mingyue Wei, Hengchang Wang, Lang Lin, Fengying Fan, Xiaoying Feng, Ping Zhang, Feng Gao, Rare-earth zirconate high-entropy nanofibrous porous ceramics for high-temperature thermal insulation applications, J. Eur. Ceram. Soc. 43 (16) (2023) 7635–7643.
[34] L. Shang, D. Wu, Y. Pu, H. Wang, F. Wang, Z. Gao, Experimental research on thermal insulation performance of lightweight ceramic material in oxidation environment up to 1700°C, Ceram. Int. 42 (2016) 3351–3360.
[35] K. Yuan, X. Wang, H. Liu, C. Feng, B. Liu, N. Cai, X. Lin, L. Zhu, G. Zhang, D. Xu, Formation of barium zirconate fibers for high-temperature thermal insulation applications, J. Am. Ceram. Soc. 99 (2016) 2913–2919.
[36] N. Erdman, D.C. Bell, R. Reichelt, Scanning electron microscopy, in: P. Hawkes, J. C. Spence (Eds.), Springer Handbook of Microscopy, Springer International Publishing, 2019, pp. 229–318.
[37] Á. Lakatos, A. Csík, Multiscale thermal investigations of graphite doped polystyrene thermal insulation, Polymers 14 (2022) 1606.
[38] H. Liu, J. Liu, Y. Tian, X. Wu, Z. Li, Investigation of high temperature thermal insulation performance of fiber-reinforced silica aerogel composites, Int. J. Therm. Sci. 183 (2023) 107827. ISSN 1290-0729.
[39] K. Wu, Q. Zhou, J. Cao, Z. Qian, B. Niu, D. Long, Ultrahigh-strength carbon aerogels for high temperature thermal insulation, J. Colloid Interface Sci. 609 (2022) 667–675. ISSN 0021-9797.
[40] Ákos Lakatos, Stability investigations of the thermal insulating performance of aerogel blanket, Energ. Build. 185 (2019) 103–111.
[41] B.P. Jelle, Accelerated climate ageing of building materials, components and structures in the laboratory, J. Mater. Sci. 47 (2012) 6475–6496.
[42] Han Guo, Jingyi Sun, Jing Ge, Dingbo Han, Yarong Lv, Hu Ping, Ce Wang, Yong Liu, Flexible mullite nanofiber membranes with high-temperature resistance and excellent thermal insulation, Ceram. Int. 50 (3) (2024) 4936–4944. Part A.
[43] Jianyu Wang, Hongyan Li, Hongli Liu, Lu Le, Tao Wang, "finger coral-like" ceramic fiber aerogels with enhanced high-temperature thermal insulation, anti-oxidation, and mechanical performance, Compos. Sci. Technol. 225 (2022) 109515.
[44] Abhijeet D. Goswami, Dnyaneshwar G. Shinde, Sakshi Singh, Ananda J. Jadhav, Dipak V. Pinjari, Enhancing the hydrophobicity of the mineral wool through surface modification with organo-silane, J. Indian Chem. Soc. 100 (10) (2023) 101085.
[45] Fengqi Liu, Yonggang Jiang, Junzong Feng, Liangjun Li, Jian Feng, Dual template strategy to prepare ultralight and high-temperature resistant ceramic nanorod aerogels for efficient thermal insulation, Ceram. Int. 49 (14) (2023) 22677–22689. Part A.
[46] Buyue Zhao, Yonghai Wang, Haiming Huang, Preparation and characterization of novel lightweight Y2Si2O7 fibrous porous ceramics for high temperature thermal insulation, Ceram. Int. 50 (11) (2024) 18510–18518. Part A.
[47] Yueqi Shao, Xu Jie, Mingyue Wei, Hengchang Wang, Lang Lin, Fengying Fan, Xiaoying Feng, Ping Zhang, Feng Gao, Rare-earth zirconate high-entropy nanofibrous porous ceramics for high-temperature thermal insulation applications, J. Eur. Ceram. Soc. 43 (16) (2023) 7635–7643 (ISSN 0955-2219.).
[48] ISO 14040:2006 Environmental management — Life cycle assessment — Principles and framework.
[49] ISO 14044:2006 Environmental management — Life cycle assessment — Requirements and guidelines.
[50] PR'e Sustainability, Life Cycle Assessment (LCA) explained. https://pre-sustainability.com/articles/life-cycle-assessment-lca-basics/ (visited on 17th Jan. 2024).
[51] Laura Golsteijn, Life Cycle Assessment (LCA) explained. https://pre-sustainability.com/articles/life-cycle-assessment-lca-basics/ (accessed: 18.06.2024).
[52] Insulfract thermal insulation, Product information sheet. https://fssperry.com/wp-content/uploads/2013/04/Insulfrax-Paper-Product-Data-Sheet.pdf (last entered in August 2024).
[53] CML-IA method. http://cml.leiden.edu/software/data-cmlia.html (last entered in August 2024).